Gallium arsenide 55Fe X-ray-photovoltaic battery

Article (Published Version)

AIP Journal of Applied Physics

Gallium arsenide 55Fe X-ray-photovoltaic battery

S. Butera, G. Lioliou, and A. M. Barnett

Citation: Journal of Applied Physics **119**, 064504 (2016); doi: 10.1063/1.4941535
View online: http://dx.doi.org/10.1063/1.4941535
View Table of Contents: http://scitation.aip.org/content/aip/journal/jap/119/6?ver=pdfcov
Published by the AIP Publishing

JOURNAL OF APPLIED PHYSICS 119, 064504 (2016)

Gallium arsenide ^{55}Fe X-ray-photovoltaic battery

S. Butera,[a] G. Lioliou, and A. M. Barnett
Semiconductor Materials and Device Laboratory, School of Engineering and Informatics, University of Sussex, Brighton BN1 9QT, United Kingdom

(Received 22 December 2015; accepted 26 January 2016; published online 10 February 2016)

The effects of temperature on the key parameters of a prototype GaAs ^{55}Fe radioisotope X-ray microbattery were studied over the temperature range of −20 °C to 70 °C. A p-i-n GaAs structure was used to collect the photons from a 254 Bq ^{55}Fe radioisotope X-ray source. Experimental results showed that the open circuit voltage and the short circuit current decreased with increased temperature. The maximum output power and the conversion efficiency of the device decreased at higher temperatures. For the reported microbattery, the highest maximum output power (1 pW, corresponding to 0.4 μW/Ci) was observed at −20 °C. A conversion efficiency of 9% was measured at −20 °C. © *2016 AIP Publishing LLC*. [http://dx.doi.org/10.1063/1.4941535]

I. INTRODUCTION

A. Nuclear microbatteries

Microelectromechanical systems (MEMS) are becoming increasingly important for military,[1] aerospace,[2] and biomedical applications.[3] In many of these applications, nuclear microbatteries could be used to provide small amounts of power over long periods of time, and for this reason they have received considerable research attention.[4] Nuclear microbatteries work by converting nuclear energy to electrical energy and offer important characteristics such as high energy density, stability, and long life. The high-energy particles, released by radioactive atoms during nuclear decay, are absorbed by the microbattery conversion material generating electrical energy.[5] Conversion materials that can be incorporated in this type of compact system include diamond,[6] SiC,[7] and GaAs.[8] These wide bandgap materials offer good electronic mobility[9,10] and low leakage currents[11,12] and are radiation hard.[13] Because of their wide bandgap, they should also present higher conversion efficiency than alternative narrower bandgap materials such as silicon, since efficiency increases linearly with bandgap.[14] A radioactive source coupled with a wide bandgap material can also be used over a broad range of temperatures. This makes them potentially suitable in applications where the environment temperature can vary significantly during use. Traditional MEMS power supplies, such as chemical batteries, cannot offer all these properties (e.g., they suffer from low energy density and short lifetime), thus nuclear microbatteries have the potential to play a key role in the development of MEMS technology.

B. Beta- and alpha-voltaic microbatteries

Recently, beta- and alpha-voltaic microbatteries of different designs have been demonstrated. Wang *et al.*[8] demonstrated different types of beta-voltaic microbatteries using Si and GaAs as converter materials. At 20 °C, the highest experimental conversion efficiencies were observed for the ^{147}Pm-Si and ^{63}Ni-GaAs microbatteries, and their values were around 0.05% and 0.075%, respectively. Another material that can be used as converter material is SiC; Chandrashekhar *et al.* proved a ^{63}Ni-SiC microbattery with at least 6% efficiency,[14] whilst Eiting *et al.* proved a ^{33}P-SiC microbattery with 4.5% efficiency.[15] Bormashov *et al.*[6] reported a ^{63}Ni-diamond beta-voltaic microbattery and a ^{238}Pu-diamond alpha-voltaic microbattery with conversion efficiencies as high as 0.6% and 3.6%, respectively, at room temperature. A rapid degradation in the alpha battery was observed due to radiation induced defect creation caused by the high-energy particles. Since the energy conversion cell was continuously irradiated by high-energy particles, the degradation effect, due to radiation-induced damage in the lattice structure, must be considered in microbattery design. The use of radioisotope alpha and beta sources in many cases can degrade the performance of the microbattery; in these situations, other solutions, which reduce device damage risk resulting in a substantially increased lifetime, have to be considered. An alternative radioactive isotope that would avoid this problem is the electron capture X-ray emitter ^{55}Fe. However, this comes at the cost of lower specific energy per Curie compared with other higher energy alpha- and beta-emitters (e.g., 0.017 μW g/(Ci cm^2) for ^{55}Fe and 0.3 μW g/(Ci cm^2) for the beta emitter ^{147}Pm).[5] This type of X-ray microbattery has the advantage of reduced device damage risk due to the low energy photons emitted and can be easily shielded providing safer working conditions.

This paper reports initial characterisation of a prototype GaAs ^{55}Fe radioisotope microbattery, using a custom GaAs photodiode originally intended for soft X-ray photon counting spectroscopy. X-ray photons, emitted by the ^{55}Fe radioisotope X-ray source, were directly converted into electrical energy using the GaAs device. The effect of temperature on the key parameters of the X-ray-photovoltaic microbattery is reported over the temperature range of −20 °C to 70 °C.

II. MATERIALS AND METHOD

A. Radioactive source and energy conversion device

An ^{55}Fe radioisotope X-ray source (Mn Kα = 5.9 keV, Mn Kβ = 6.49 keV), activity 254 MBq, was positioned 5 mm

[a]Author to whom correspondence should be addressed. Electronic mail: S.Butera@sussex.ac.uk.

above the top of the 400 μm diameter p-i-n GaAs mesa X-ray photodiode. The GaAs epilayer of the device was grown to the Authors' specifications by the EPSRC National Centre for III-V Technologies at the University of Sheffield, UK, by metalorganic chemical vapour deposition (MOCVD) on a commercial GaAs n^+ substrate. The doping concentration of the p and n layers was 2×10^{18} cm^{-3}. The layers' thicknesses were 0.5 μm for the p^+-region, 10 μm for the i-region, and 1 μm for the n^+-region. After growth, the wafer was processed to form mesa structures using 1:1:1 H_3PO_4:H_2O_2:H_2O solution followed by 10 s in 1:8:80 H_2SO_4:H_2O_2:H_2O solution. The GaAs mesa devices were unpassivated. An Ohmic rear contact consisting of 20 nm of InGe and 200 nm of Au was evaporated onto the rear of the substrate and an Ohmic top contact consisting of 20 nm of Ti and 200 nm of Au was evaporated on the p^+-side of the mesa device. The top Ohmic contact covered 33% of the surface of the photodiode. Subsequent characterisation was performed at University of Sussex, UK. The device layers, their relative thicknesses, and materials were summarised in Table I.

Using the Beer-Lambert law and assuming complete charge collection in the i-layer, X-ray quantum efficiencies (QE_{NC}) of 57% and 48% were calculated for the device for the 5.9 keV and 6.49 keV photons, respectively, assuming a dead region close to the top surface with a width of 0.16 μm.[12,16] These values decreased to 48% and 42%, respectively, considering the attenuations of the photons through the top metal contact (QE_C). However, since the top metal contact only covered the 33% of the device surface, the total device QE was calculated from a weighted sum of QE_{NC} and QE_C. This gave values for the X-ray total device quantum efficiency of 54% and 46% for the 5.9 keV and 6.49 keV photons, respectively. The GaAs attenuation coefficients at 5.9 keV and 6.49 keV used to calculate the quantum efficiency were taken after Ref. 16, whilst the Ti and Au attenuation coefficients at 5.9 keV and 6.49 keV were taken after Ref. 17. Total device QE greater than 90% may be obtained by increasing the i-layer thickness to 40 μm; this i-layer thickness can be achieved using chemical vapor phase deposition (CVPD) techniques as demonstrated by Owens *et al.*[18] An advantage of the reported X-ray microbattery prototype is the use of the ^{55}Fe radioisotope X-ray source, a radioisotope which is readily available.

TABLE I. Layer details of the GaAs X-ray photodiode.

Layer	Material	Thickness (μm)	Dopant	Dopant type	Doping density (cm^{-3})
1	Ti	0.02			
2	Au	0.2			
3	GaAs	0.5	Be	p^+	2×10^{18}
4	GaAs	10	Undoped		$<10^{15}$
5	GaAs	1	Si	n^+	2×10^{18}
6	Substrate n^+ GaAs				
7	Au	0.2			
8	InGe	0.02			

The GaAs ^{55}Fe radioisotope X-ray microbattery works by directly converting the incident X-rays to electron-hole pairs as a consequence of the photoelectric effect. Because of the combination of built-in and applied electric field, electrons and holes in the depletion region accelerate in opposite directions and are swept to the p^+-type and n^+-type regions, respectively, generating a photocurrent. The average energy consumed in the generation of an electron-hole pair is called the electron–hole creation energy (4.18 eV for GaAs[19]).

B. Experiment and measurements

To control the ambient temperature and humidity, the X-ray microbattery was placed inside a TAS Micro MT climatic cabinet in a dry nitrogen atmosphere (relative humidity <5%). Dark and illuminated current characteristics of the GaAs device were measured as functions of applied bias and temperature. Forward bias measurements from 0 V to 0.4 V were made in 0.005 V increments using a Keithley 6487 picoammeter/voltage source and are shown in Fig. 1. The uncertainty associated with the current readings was 0.3% of their values plus 400 fA, while the uncertainty associated with the applied biases was 0.1% of their values plus 1 mV.[20]

As was expected, greater electric fields across the i-region led to higher currents in the GaAs device. The dark current increased exponentially as a function of applied bias ($\propto \exp\{qV/nkT\}$, where n is the ideality factor, k is the Boltzmann constant, and T is the temperature).[9] A linear least squares fit, at 20 °C, showed that natural logarithm of the dark current was linearly dependent on the applied forward bias with a slope (22.74 ± 0.04) A V^{-1}; this led to an observed ideality factor of 1.739 ± 0.003. Because the ideality factor was close to 2, it was possible to conclude that generation-recombination current was dominant over the diffusion current in the device. When the device was illuminated by the ^{55}Fe radioisotope X-ray source, the total current through the device was the sum of the dark current and the photocurrent: the illuminated current curve as a function of forward bias (filled circles in Fig. 1) was shifted with respect to the dark current (empty squares in Fig. 1). The

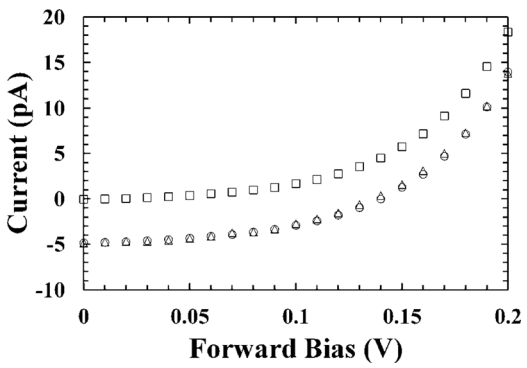

FIG. 1. Measured current as a function of applied forward bias, at 20 °C, when the GaAs detector was in the dark (empty squares) and illuminated by the ^{55}Fe radioisotope X-ray source (empty circles). Also shown (empty triangles) are the expected illuminated current values; these were computed calculating the changes in photocurrent due to the decreased electric field within the detector.

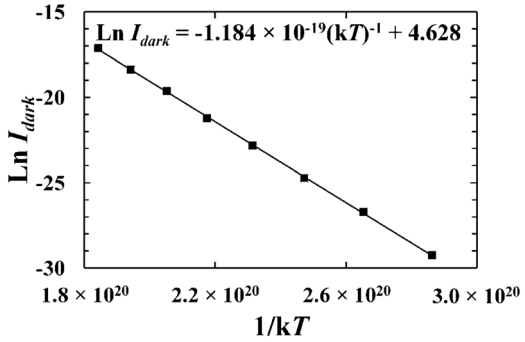

FIG. 2. Measured dark current as a function of temperature (squares). Also shown is the line of the best fit computed by linear least squares fitting.

photocurrent decreased with increased voltage from 0 V to 0.2 V: the observed decrease was (0.3 ± 0.8) pA at 20 °C. Whilst the measured decrease was smaller than its uncertainty, some decrease was expected due to the lower electric field and consequently lower electron velocity at higher applied forward bias.[21] The expected photocurrent due to the decreased electric field within the detector[9] is also shown in Fig. 1 (empty triangles). The expected photocurrent behaviour was comparable with that from the experiment: the expected decrease in photocurrent between 0 V and 0.2 V was computed to be 0.4 pA.

To characterise the temperature dependence of the performance of the system, the microbattery's temperature was varied from 70 °C to −20 °C. As expected, the dark current of the GaAs device increased exponentially as a function of temperatures ($\propto \exp\{-E_g/n\mathrm{k}T\}$, where E_g is the bandgap, n is the ideality factor, and k is the Boltzmann constant).[9] Higher dark currents were observed at high temperature due to the higher thermal energy available. In Fig. 2, the natural logarithm of the dark current as a function of 1/kT was plotted, for 0.2 V forward bias. A linear least squares fit showed a linear dependence with a slope of $(1184 \pm 8) \times 10^{-22}$ J $(0.739 \pm 0.005$ eV). The observed slope was around half of the GaAs bandgap. Thus, the generation-recombination mechanism was considered dominant over the diffusion mechanism, for all temperatures measured.

The saturation current (I_0) was also extrapolated from the dark current of the GaAs device as a function of forward bias.[7] Fig. 3(a) shows the linear least square fit used to extrapolate the saturation current at 20 °C, whilst Fig. 3(b) shows the measured relationship between the logarithm of the saturation current and the temperature.

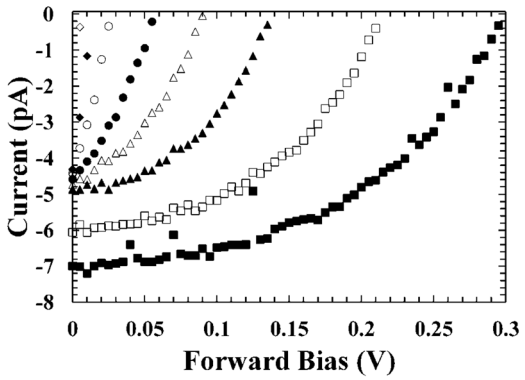

FIG. 4. Measured currents as a function of applied forward bias when the GaAs detector was illuminated by the ^{55}Fe radioisotope X-ray source at 70 °C (empty rhombuses), 60 °C (filled rhombuses), 50 °C (empty circles), 40 °C (filled circles), 30 °C (empty triangles), 20 °C (filled triangles), 0 °C (empty squares), and −20 °C (filled squares).

As can be seen in Fig. 3, the magnitude of the observed natural logarithm of the saturation current decreased at higher temperatures. From 20 °C to 60 °C, this decrease was 9.36 ± 0.07. For a simple pn diode, where recombination-generation mechanisms are predominant, the saturation current is given by

$$I_s = \frac{qx_d\sqrt{N_C N_V}}{2\tau_n}\exp\left(-\frac{E_g}{2\mathrm{k}T}\right), \quad (1)$$

where N_C and N_V are the effective density of states in the conduction and valence bands, respectively, x_d is the depletion width, τ_n is the minority electron lifetime, E_g is the bandgap, and k is the Boltzmann constant.[22]

With the assumption that the $-E_g/2kT$ term in Eq. (1) dominated the temperature dependence of the saturation current, the expected decrease between 60 °C and −20 °C was calculated to be 8.56. This value is remarkably similar to the experimental value (9.36 ± 0.07) considering that the approximation does not include the temperature dependences of the other terms in Eq. (1).

The measured currents as a function of applied forward bias when X-ray-photovoltaic microbattery was illuminated by the ^{55}Fe radioisotope X-ray source at different temperatures are shown in Figure 4.

As shown in Fig. 4, the softness in the knee of the measured current as a function of applied forward bias decreased with increasing temperature. The experimental values of the open circuit voltage (V_{OC}) and the short circuit current (I_{SC})

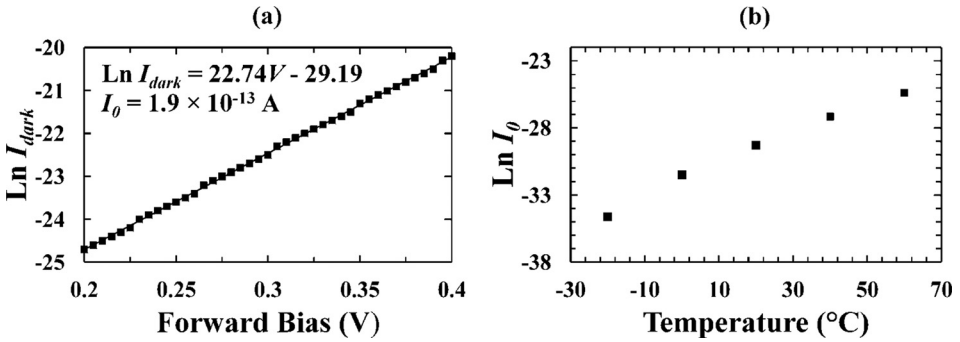

FIG. 3. (a) Dark current as a function of applied forward bias at 20 °C. A linear fit on the data was used to calculate the correspondent saturation current. (b) The logarithm of the saturation current as a function of temperature.

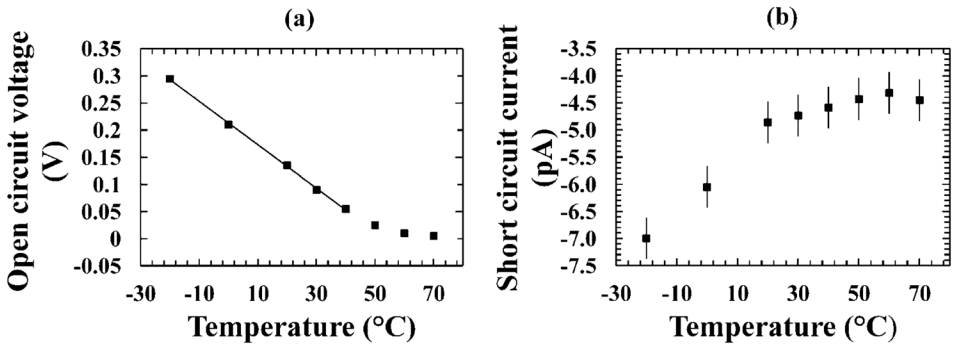

FIG. 5. (a) Open circuit voltage (V_{OC}) as a function of temperature. (b) Short circuit current (I_{SC}) as a function of temperature.

were obtained as the interception point of the curves in Fig. 4 on the vertical and horizontal axes, respectively. Fig. 5 shows V_{OC} and I_{SC} as functions of temperature.

The open circuit voltage (V_{OC}) was measured to decrease with temperature. The observed behaviour presented in Fig. 5 was explained considering that the open circuit voltage increases logarithmically with decreasing saturation current.[9] At temperatures lower than 40 °C, a linear relationship between the open circuit voltage and temperature was observed. In this temperature range, a linear least squares fit showed that V_{OC} was dependent on temperature (T) according the relation $V_{OC} = -AT + B$ with $A = (0.00400 \pm 0.00007)$ V °C^{-1} and $B = (0.213 \pm 0.002)$ V. It should be noted that the open circuit voltage increases with bandgap, so to obtain a larger V_{OC}, a larger bandgap material is preferred.[9] In contrast with what may have been expected, the experimental short circuit current (I_{SC}) magnitude decreases with increasing temperature. Because of the greater average energy consumed in the generation of an electron-hole pair (electron-hole creation energy) at low temperatures,[19] less current may have been expected at low temperatures compared with high temperatures. The different behaviours observed may have been attributed to the increased electron mobility at lower temperatures.[9] As the temperature increased, thermal vibrations (phonons) within the semiconductor increased and caused increased scattering that resulted in lower carrier mobilities. The decrease in carrier mobility was expected to be proportional to $T^{-3/2}$;[9] this resulted in an expected decrease in short circuit current of 2.6 pA between −20 °C and 70 °C. This value was in agreement with the observed decrease in I_{SC} that was measured to be (2.5 ± 0.5) pA. A similar behaviour to that observed in Fig. 5 has been reported previously.[23]

The output power of the X-ray-photovoltaic microbattery was calculated as $P = IV$. We defined I_m and V_m as the values of current and voltage correspondent to the maximum power output P_m ($=I_mV_m$), respectively. In Fig. 6(a), P as a function of forward bias is shown. The output power increased to a maximum, P_m (corresponding to V_m and I_m) and then decreased. In Fig. 6(b), the magnitude of the measured maximum power at each temperature is reported: as the temperature increased, the magnitude of the maximum output power decreased. This behavior was due to the significant decrease in V_m (itself dependent on the open circuit voltage[9]) with respect to temperature. A maximum output power of 1 pW, corresponding to 0.4 μW/Ci, was measured at −20 °C. The microbattery's maximum output power may be improved in the next prototype generation with a better system design where most of the photons emitted by the ^{55}Fe radioisotope X-ray source (activity 254 MBq) are collected: in the reported design, only 0.1% of the emitted photons impinged on the surface of the GaAs device. The incident X-ray flux was estimated by knowing the activity of the source, the emission probabilities of Mn Kα and Mn Kβ X-rays from ^{55}Fe (0.245 and 0.0338, respectively[24]), the thickness of the radioisotope X-ray source's Be window (0.25 mm), and the geometry of the source and detector.

The conversion efficiency (η) defined as the ratio in percentage terms between the maximum measured power output and the maximum power that would be obtainable from the X-ray photons usefully absorbed by the device if the device conversion efficiency was 100% is shown in Fig. 7. The highest value for η (9%) was observed at −20 °C.

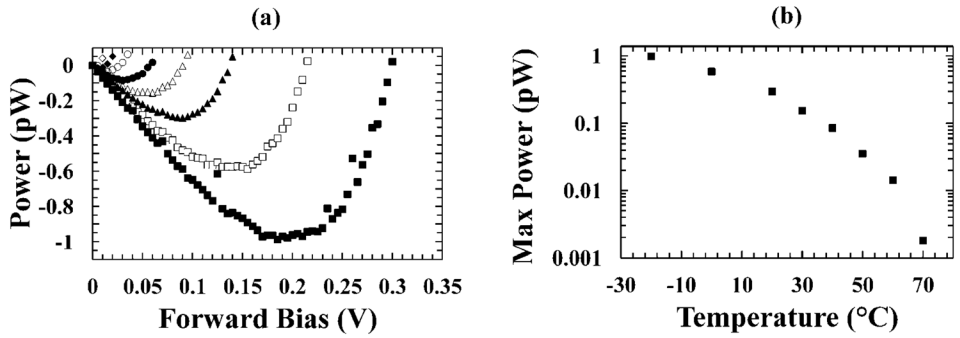

FIG. 6. (a) X-ray microbattery output power as a function of applied forward bias at 70 °C (empty rhombuses), 60 °C (filled rhombuses), 50 °C (empty circles), 40 °C (filled circles), 30 °C (empty triangles), 20 °C (filled triangles), 0 °C (empty squares), and −20 °C (filled squares). (b) Experimental maximum power as a function of temperature.

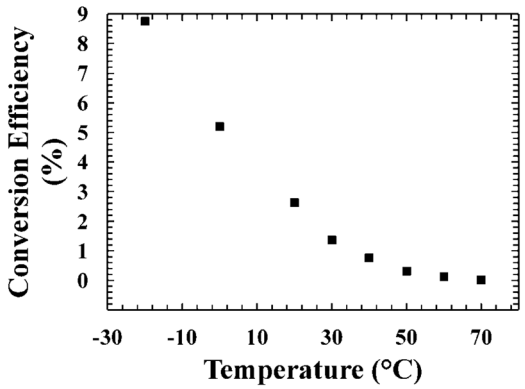

FIG. 7. Conversion efficiency (η) as a function of temperature.

III. CONCLUSION

In this paper, an ^{55}Fe radioisotope X-ray source (activity 254 MBq) and a GaAs photodetector were used to build a prototype X-ray-photovoltaic microbattery. Because GaAs growth and processing techniques are relatively cheap and more routinely available than some alternative wide bandgap materials, this type of microbattery may provide cost efficiency benefits in the development of microbatteries for MEMS technology and other applications. The reported ^{55}Fe-GaAs system was characterised as a function of temperature (from $-20\,^{\circ}$C to $70\,^{\circ}$C). The saturation current increased with increased temperature. The open circuit voltage, the maximum power, and the conversion efficiency values increased with decreased temperature. In contrast with what may have been expected, the short circuit current magnitude decreased at high temperature; this behaviour has been also observed by other researchers.[23] The highest maximum output power observed for the microbattery was 1 pW (corresponding to 0.4 μW/Ci) at $-20\,^{\circ}$C. The microbattery maximum output power can be improved in the next prototype generation with a better system design: in the reported design, only 0.1% of photons emitted by the ^{55}Fe radioisotope X-ray source impinged the surface of the GaAs device. The conversion efficiency of the battery, taking into account attenuation from contacts and dead layer, was around 9% at $-20\,^{\circ}$C. Attenuation of the X-ray photons within the radioactive source itself will also have resulted in an underestimation of conversion efficiency values.

ACKNOWLEDGMENTS

This work was supported by STFC Grant No. ST/M002772/1 (University of Sussex, A.M.B., PI). The authors are grateful to B. J. Stevens, R. J. Airey, and S. Kumar at the EPSRC National Centre for III-V Technologies for material growth and fabrication. G. Lioliou acknowledges funding received from University of Sussex in the form of a Ph.D. scholarship.

[1]X. Lee and C. Wang, Appl. Opt. **54**, 2219 (2015).
[2]J. H. Park, G. K. Garipov, J. A. Jeon, B. A. Khrenov, J. E. Kim, M. Kim, Y. K. Kim, C.-H. Lee, J. Lee, G. W. Na, S. Nam, I. H. Park, and Y.-S. Park, Opt. Express **16**, 20249 (2008).
[3]M. Birkholz, K.-E. Ehwald, T. Basmer, P. Kulse, C. Reich, J. Drews, D. Genschow, U. Haak, S. Marschmeyer, E. Matthus, K. Schulz, D. Wolansky, W. Winkler, T. Guschauski, and R. Ehwald, J. Appl. Phys. **113**, 244904 (2013).
[4]P. B. Koeneman, I. J. Busch-Vishniac, and K. L. Wood, J. Microelectromech. Syst. **6**, 355 (1997).
[5]K. E. Bower, Y. A. Barbanel, Y. G. Shreter, and G. W. Bohnert, *Polymers, Phosphors, and Voltaics for Radioisotope Microbatteries* (CRC Press LLC, Boca Raton, 2002).
[6]V. Bormashov, S. Troschiev, A. Volkov, S. Tarelkin, E. Korostylev, A. Golovanov, M. Kuznetsov, D. Teteruk, N. Kornilov, and S. Terentiev, Phys. Status Solidi A **212**, 2539 (2015).
[7]X.-Y. Li, Y. Ren, X.-J. Chen, D.-Y. Qiao, and W.-Z. Yuan, J. Radioanal. Nucl. Chem. **287**, 173 (2011).
[8]H. Wang, X.-b. Tang, Y.-P. Liu, Z.-H. Xu, M. Liu, and D. Chen, Nucl. Instrum. Methods Phys. Res., Sect. B **359**, 36 (2015).
[9]S. M. Sze and K. K. Ng, *Physics of Semiconductor Devices*, 3rd ed. (John Wiley & Sons, New Jersey, 2007).
[10]W. Choyke and G. Pensl, MRS Bull. **22**, 25 (1997).
[11]G. Lioliou, M. Mazzillo, A. Sciuto, and A. M. Barnett, Opt. Express **23**, 21657 (2015).
[12]G. Lioliou, X. Meng, J. S. Ng, and A. M. Barnett, Nucl. Instrum. Methods Phys. Res., Sect. A **813**, 1–9 (2016).
[13]E. Monroy, F. Omnès, and F. Calle, Semicond. Sci. Technol. **18**, R33 (2003).
[14]M. Chandrashekhar, C. I. Thomas, H. Li, M. G. Spencer, and A. Lal, Appl. Phys. Lett. **88**, 033506 (2006).
[15]C. J. Eiting, V. Krishnamoorthy, S. Rodgers, and T. George, Appl. Phys. Lett. **88**, 064101 (2006).
[16]D. T. Cromer and D. Liberman, J. Chem. Phys. **53**, 1891 (1970).
[17]J. H. Hubbell, Int. J. Appl. Radiat. Isot. **33**, 1269 (1982).
[18]A. Owens, M. Bavdaz, A. Peacock, A. Poelaert, H. Andersson, S. Nenonen, L. Troger, and G. Bertuccio, Nucl. Instrum. Methods Phys. Res., Sect. A **466**, 168 (2001).
[19]G. Bertuccio and D. Maiocchi, J. Appl. Phys. **92**, 1248 (2002).
[20]Keithley Instruments, Inc., *Model 6487 Picoammeter/Voltage Source Reference Manual*, 6487-901-01 Rev B (Cleveland, 2011).
[21]J. Blakemore, J. Appl. Phys. **53**, R123 (1982).
[22]M. V. S. Chandrashekhar, R. Duggirala, M. G. Spencer, and A. Lal, Appl. Phys. Lett. **91**, 053511 (2007).
[23]S. Krawczyk, A. Jakubowski, and M. Żurawska, Sol. Cells **4**, 187 (1981).
[24]U. Schotzig, Appl. Radiat. Isot. **53**, 469 (2000).